TOUGH2/iTOUGH2 MODELING IN SUPPORT OF THE GAS MIGRATION TEST (GMT) AT THE GRIMSEL TEST SITE (SWITZERLAND)

Rainer Senger, INTERA Incorporated, 9111A Research Blvd., Austin, Texas 78757, rsenger@intera.com
Bill Lanyon, Fracture Systems Ltd, Tregurrian, St Ives, Cornwall, UK, bill@fracture-systems.co.uk
Paul Marschall, NAGRA, Hardstrasse 73, CH-5430 Wettingen, Switzerland, paul.marschall@nagra.ch
Stratis Vomvoris, NAGRA, Hardstrasse 73, CH-5430 Wettingen, Switzerland, stratis.vomvoris@nagra.ch
Kenichi Ando, RWMC, N0.15 Mori Bldg.,2-8-10,Toranomon,Minato-ku,Tokyo, Japan k-ando@rwmc.or.jp

ABSTRACT

The Gas Migration Test (GMT) is being performed at the Grimsel Test Site (GTS) underground research facility in central Switzerland. The GMT is designed to investigate gas migration through an engineered barrier system (EBS). The EBS consists of a concrete silo embedded in a sand/bentonite buffer emplaced in a silo cavern that intersects a shear zone in the surrounding granite host rock. The GMT is instrumented by a detailed monitoring system consisting of pressure transducers, total pressure cells, and Time Domain Reflectometers that were installed in the EBS and in the adjacent geosphere.

The in-situ experiment has involved several stages: (1) site selection and characterization, (2) excavation of the access drift and silo cavern, (3) construction and instrumentation, (4) saturation of the EBS by natural water inflow and by water injection (ca. 12 months), and (5) hydraulic testing of the EBS prior to gas generation (2 months). These stages are now complete and ongoing and future stages include: (6) long-term gas generation inside the concrete silo (6 to 9 months), (7) post-gas hydraulic testing (2 months), and (8) dismantling (4 months). At the end of gas generation, a gas tracer will be added to visualise gas flow paths using a reactive gas tracer.

The design of the experimental set-up and the experimental procedures were tested and refined with a design model implemented with the TOUGH2 code. Different saturation strategies were investigated with the design model that incorporated the detailed geometry of the EBS and surrounding host rock. In addition to optimizing the saturation procedure of the EBS and subsequent gas injection phase, iTOUGH2 modeling was used to calibrate various hydraulic parameters of the EBS based on the monitored response during the saturation phase.

Hydrotest results (Stage 5 above) were analyzed with iTOUGH2 to further calibrate the hydraulic properties of the EBS materials and determine potential changes in properties during saturation. These updated properties were then implemented in the TOUGH2 design model to optimize the long-term gas generation phase by defining the gas injection

rates or possible variations in gas injection rates. The combination of TOUGH2 design modeling and iTOUGH2 calibration of hydraulic and two-phase flow properties has been crucial for the development and optimization of the GMT experiment.

INTRODUCTION

The Gas Migration Test (GMT) is an experiment concerning gas migration in an Engineered Barrier System (EBS). Gas migration from a radioactive waste repository is a critical issue for intermediate level wastes (ILW) in some national radioactive waste programs. A typical concept for such an ILW repository is to place the waste in concrete silos embedded in a sand/bentonite buffer.

The GMT is being performed at the Grimsel Test Site (GTS) underground research facility in central Switzerland under the auspices of RWMC (Radioactive Waste Management Funding and Research Center, Japan), with the support of Nagra and Obayashi Corporation. The experimental setup consists of a concrete silo embedded in a sand/bentonite buffer, emplaced in a cavern (Figure 1). The silo cavern intersects a shear zone in the surrounding granite host rock and is separated from the access drift by a concrete plug.
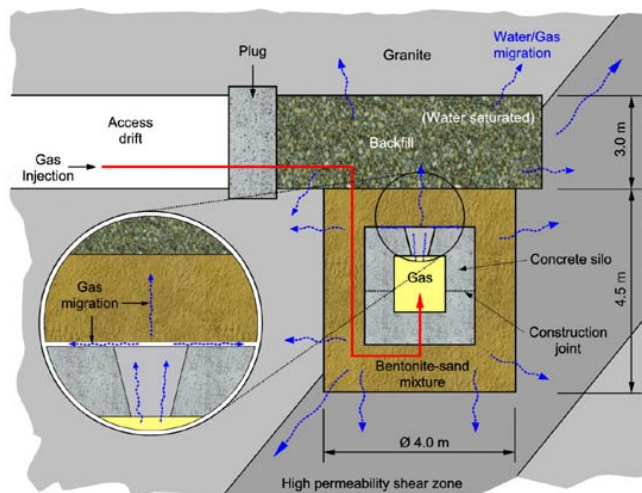

Figure 1. GMT geometry and concept.

The GMT is designed to study gas migration from the silo through the EBS and into the adjacent host rock. Specifically, the GMT investigates the relevant processes associated with gas migration, which include (1) pressure buildup associated with waste-generated gas and displacement of contaminated water from the waste silo through the EBS and into the geosphere, (2) generation of excess gas/water pressures affecting in-situ stress conditions in the concrete silo and surrounding sand/bentonite, which can impact the structural integrity of the EBS components, and (3) transport of volatile nuclides through the EBS under two-phase flow conditions and possibly affected by coupled hydro-mechanical processes. Of particular interest for the sand/bentonite buffer is the potential gas flow behavior associated with pathway dilation or interface opening when the gas pressure is close to the confining stress (Fig. 1).

The components of the GMT experiment, shown in Figure 1, consist of (1) the silo cavern, (2) the concrete silo (height 2.5 m, external diameter 2.5 m) embedded in the cavern, (3) the high-permeability mortar gas-vent in the top of the concrete silo, (4) the sand/bentonite backfill around the silo (80% sand and 20% bentonite), (5) the tunnel backfill (gravel/sand) in the upper part of the cavern, and (6) the plug separating the EBS from the access drift. Gas will be injected at the center of the concrete silo and the gas breakthrough and migration through the engineered barriers and adjacent geosphere will be monitored by a detailed monitoring system consisting of pressure transducers, total pressure cells, and Time Domain Reflectometers (TDR) installed in the EBS and adjacent geosphere.

The in-situ experiment has involved several stages over the last 5 years, which include: (1) site selection and characterization starting in 1998, (2) excavation of the access drift and silo cavern, completed in November 2000, (3) construction and instrumentation between November and July, 2001, (4) saturation of the EBS by natural water inflow and by water injection starting in August 2001 and continues to present, and (5) hydraulic testing of the EBS prior to gas generation (October - December 2002). The ongoing and future stages include: (6) long-term gas generation inside the concrete silo for 6 to 9 months (started on January 2003), (7) post-gas hydraulic testing (2 months), and (8) dismantling (4 months). At the end of gas generation, a gas tracer will be added to visualize gas flow paths using a reactive gas tracer.

In addition to the in-situ test, a laboratory program was developed for sensor testing/development and to determine hydraulic/two-phase properties of the sand/bentonite buffer. The results from the laboratory

program and previous studies by the Radioactive Waste Management Funding and Research Center (RWMC), Japan, were used as input to the modeling work.

The design of the in-situ experiment, particularly stages (4) through (7) was supported by numerical modeling using TOUGH2 (Pruess et al., 1999). Results from the saturation stage and particularly from the hydraulic testing of the EBS prior to the gas injection stage were analyzed using iTOUGH2 (Finsterle, 1993). Additional modeling studies are supported by subtask partners addressing potential hyro-mechanical phenomena in addition to the two-phase flow processes using specific codes. These codes and corresponding subtask partners include CODE-BRIGHT (ENRESA/Univ. Polytechnic of Catalunya, Spain), GETFLOW (GET Inc., Japan), MEHRLIN (ANDRA/Colenco Power Ltd., France), and ROCKFLOW (BGR, Germany).

This paper describes the design modeling and analysis with TOUGH2 focusing on the saturation stage, and the calibration of system hydraulic properties of the EBS components with iTOUGH2 based the water test (WT1) responses. The refined hydraulic parameters, particularly those for the sand/bentonite, derived from the WT1 analysis, have been used for optimizing the gas injection strategy.

THE GMT DESIGN MODEL

The GMT configuration was implemented with a radially-symmetric mesh, representing the concrete silo emplaced in the sand/bentonite buffer and overlain by the tunnel backfill (Fig. 2). The surrounding granite host rock was implemented in the radial model as a vertical plane of unit width representing the high-permeability shear zone intersecting the silo cavern (Fig. 1). The effects of the tunnel seal and the access tunnel is incorporated into the integrated finite difference (IFD) mesh through specific hydraulic connections between the upper cavern fill, the tunnel seal, and the access tunnel (Fig. 2). In addition, a specific connection between the access tunnel and the top of the cavern fill represents a gas drain, allowing only air to drain from the cavern silo during the cavern saturation, up to the point when the upper cavern becomes fully water saturated, after which the drain was closed.

In addition to properly account for the relevant processes that control gas migration for the concrete silo through the sand/bentonite and into the surrounding geosphere, the model requires incorporation of the different stages of the experiment, which include: (1) initial conditions, representing hydraulic conditions prior to the excavation of the GMT drift, (2) desaturation, representing hydraulic conditions associated with the

open GMT silo, (3) Phase-1 saturation, representing natural inflow into the EBS during the emplacement of the sand/bentonite and tunnel fill, (4) Phase-2 saturation, representing forced water injection into the EBS, (5) WT1 with continued water injection into the upper cavern, and (6) gas injection into the concrete silo with continued water injection into the upper cavern. The simulations of the different stages are performed in sequence, whereby the simulation results from the previous stage are used as initial conditions for the simulation of the subsequent stage.
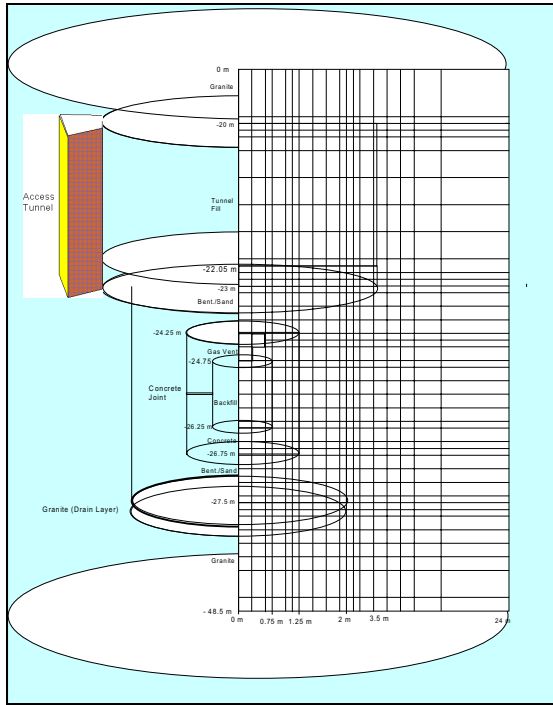
In Layers 8, 9, and 10 a lead-nitrate solution was added to the mixing water to permit visualization of the gas flow pathways after dismantling of the experiment. The addition of the lead-nitrate may have affected the swelling of the bentonite, resulting in generally higher permeabilities in Layers 8 – 10 compared to the other sand/bentonite layers (Romero et al., 2002).
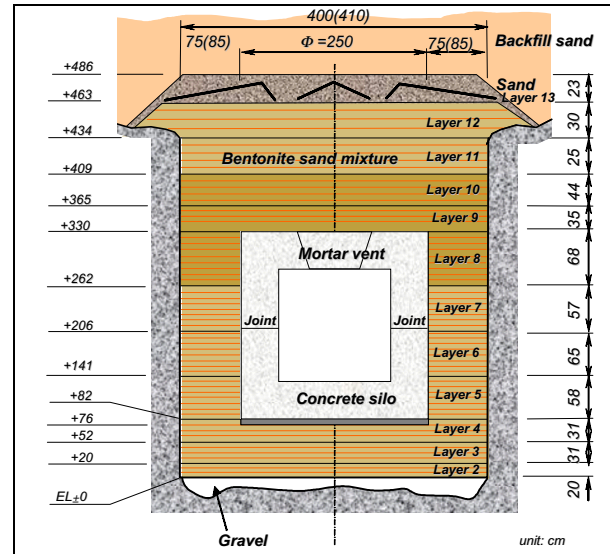

Figure 3. Detailed geometry of the EBS, showing layering of the sand/bentonite.

Figure 2. Schematic mesh geometry for the radial-symmetric EBS and the 2-D vertical plane representing the granite shear zone.

The emplacement of the sand/bentonite buffer was done in layers, each layer composed of several lifts that were compacted before the next lift was added (Fig. 3). This was done to assure uniform compaction of the sand/bentonite buffer with relatively uniform permeability in the order of 1.E-16 to 1.E-18 m^2, whereby swelling of the bentonite during saturation is expected to cause a decrease in permeability.

The numerical model incorporated the detailed geometry of the individual layers, which were represented by two or more rows of elements. Initial estimates of hydraulic and two-phase flow properties for the different EBS materials were based on the various laboratory investigations (Lanyon, 2000; Romero et al., 2002, 2003). A summary of the hydraulic and two-phase flow properties for the different EBS materials and surrounding granite host rock is given in Table 1, indicating a relatively large range in sand/bentonite permeability based on lab data and analysis of the saturation and WT1 stages, discussed below. The detailed mesh representing the different EBS materials with the distribution of the initial permeability estimates is shown in Figure 4.

Table 1. Summary of initial hydraulic and two-phase flow properties

| Unit | Hydraulic Properties | | | | Two-Phase Flow Properties | | |
	Permeability k (m^2)	Compress-ibility (Pa^{-1})	Porosity ϕ	TPF Model	Air-Entry Pressure P_{ae}(Pa)	Shape Parameter[1]	Residual Water Sat. S_{lr}
Granite (fracture)	5.E-17	3.4E-10	0.01	vG	1.E+5	n=1.88	0.10
Granite (interface)	1.E-14	3.4E-10	0.01	vG	1.E+4	n=1.88	0.10
Gravel (Layer 1)	1.E-12	1.E-8	0.30	vG	5.E+2	n=2	0.10
Sand/Bentonite:	5.E-15–5E-19	1.E-8	0.30	vG/*Corey*	2.5.E+5–1.E+4	n=2.5/λ=1	0.58/*0.3*
Concrete	1.E-18	2.7E-11	0.2	vG	1.E+6	n=2	0.25
Tunnel/Backfill	1.E-12	1.E-8	0.25	vG	5.E+2.	n=2	0.25

SATURATION STAGE

The natural water inflow into the GMT cavern through the granite shear zone was relatively small, requiring artifical saturation of the EBS by water injection into specific locations inside the EBS. After construction of the concrete silo and emplacement of the sand/bentonite to the top of the concrete silo, the silo was filled with water. The surrounding sand/bentonite material was prepared at an initial water saturation of 70% and the overlying tunnel backfill material was at an initial saturation of 30%. Because of the relatively low confining stress of the EBS, borne by the weight of the tunnel backfill, the potential differential pressure increase associated with water injection into the silo was limited to less than 40 kPa.

In a series of simulations the design model was used to evaluate different water-injection strategies to achieve saturation of the sand/bentonite buffer. In the first stage of the field test, water was injected into the gravel layer at the bottom of the silo. The pressure response was used to get an initial estimate of the effective permeability of the overlying sand/bentonite. The results indicated relatively low permeabilities (less than 1.E-18 m^2) for the lower layers. Based on these results, the injection strategy was modified such that the main water injection continued along the outer edge at the base of the upper cavern. This resulted in relatively rapid saturation of the tunnel fill and associated pressure buildup in the upper cavern.

The pressure and saturation responses from water injection into the upper cavern indicated relatively rapid pressure responses in Layers 8 – 10 and little or no responses in Layers 2 – 7 and 11 - 12. Because the pressure transducers and TDRs are installed mainly at the top of the individual layers, different conceptual models have been considered for the sand/bentonite (Fig. 4): (1) In the uniform-K model, the higher permeability is uniform within Layers 8 – 10; (2) in the high-K tops model, the high permeability occurs only in the top lift within Layers 8 – 10, resulting from drying of the exposed top lifts; (3) in a third model, the high permeability is localized within the top lifts along interfaces between the instrumentation arms and the sand/bentonite, which may have opened due to uneven compaction of the sand/bentonite layers. A preliminary, fully 3-D numerical mesh was set up for the third model concept, but no detailed simulations have yet been performed.
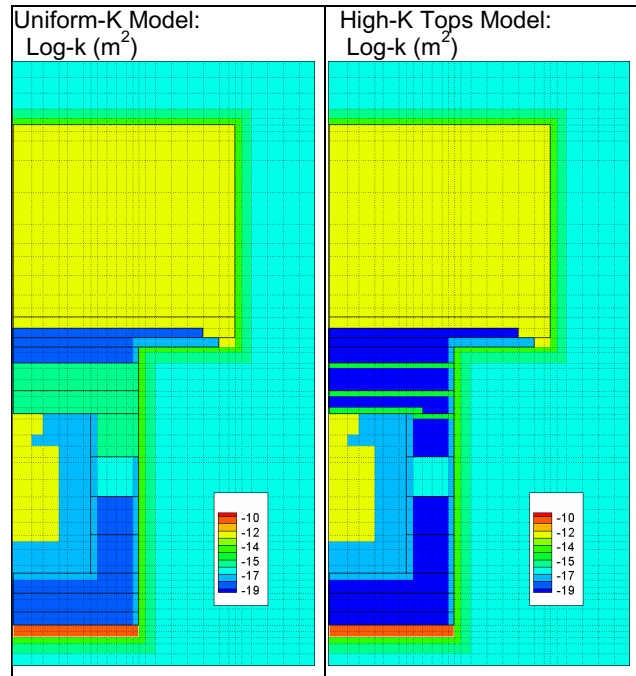

Figure 4. Conceptual models for the sand/bentonite: Uniform-K for Layers 8 – 10, and High-K for top lifts in Layers 8 – 10.

The pressure and saturation responses for selected transducers in Layers 8 and 11, are shown in Figure 5. The observed pressures indicate a gradual increase during the early saturation stages prior to January 2002. After the upper cavern backfill became fully water saturated and the system became "confined", the pressures in the high-K sand/bentonite layers show a rapid increase whereas pressures in the low-K layers only indicate a moderate increase. The variability in the pressure response in the high-K layers is due to fluctuations in the water injection rate in the upper cavern. These fluctuations caused variations in the upper cavern pressure, which are readily transmitted to the high-K sand/bentonite layers. These fluctuations in cavern pressure are not accounted for in the modeling; instead, a constant pressure was assumed for the upper cavern starting in February 2002 (Fig. 5). The simulated pressure compare reasonably well with the measured data for both the high-K and low-K layers.

The inferred saturations from the TDR measurements also show different responses between the high-K layers and the low-K layers. Both indicate a distinct response associated with the pressurization of the upper cavern fill. The sudden change in saturation, particularly for the low-K layers may be due to compaction resulting in an effective increase in water saturation.

- 5 -

The simulations with the high-K tops model for the sand/bentonite layers yielded similar results, whereby the saturation in top lifts of the high-K layers increased earlier due to the higher permeability assumed for the top lifts in Layers $8 - 10$ (5.E-15 m^2) compared to the permeability (1.E-15 m^2) used in the uniform-K model for Layers $8 - 10$.

The simulated distributions of saturation and water fluxes (left) and pressure and gas fluxes (right) at different times during the saturation phase are shown at the bottom in Figure 5 for the uniform-K model. The first time frame (11/26/01) indicates the filling of the upper cavern with water indicating small saturation increases in the high-K layers.
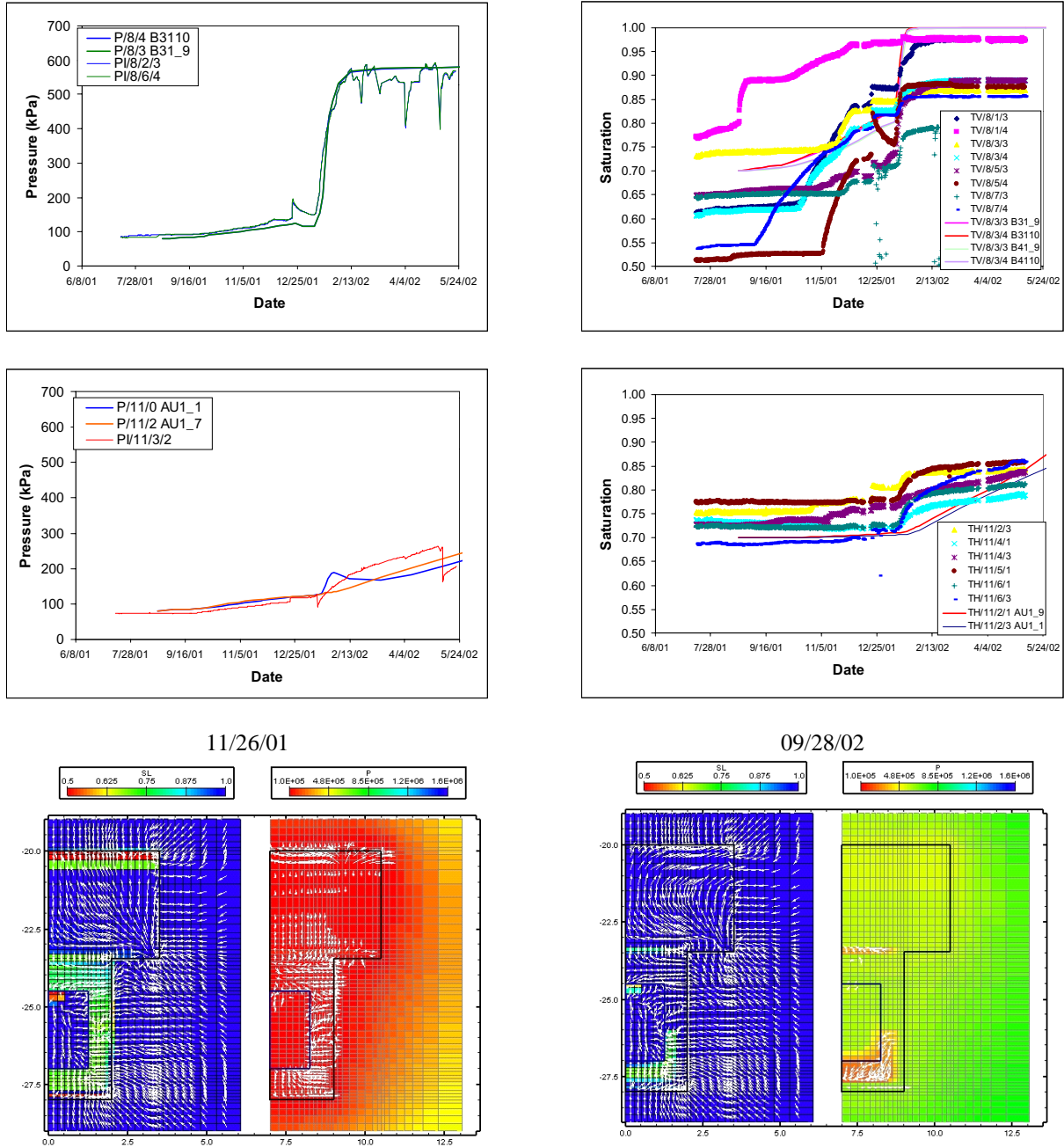

Figure 5. Measured and simulated pressure and saturation response in Layer 8 (high-K) and in Layer 11 (low-K) and simulated distribution of saturation, pressure, and gas/water flow using the uniform-K model.

The top layers (Layers 11-12) and the bottom layers (Layers 2 – 6) indicate no changes. At the end of the saturation stage (September 2002), the high-K layers appear to be fully water saturated (i.e., no gas flow) whereas the top two layers and particularly the bottom layers indicate partial saturation with significant amounts of remaining air. Even though the high-K layers indicate no gas flux above the silo, the simulation indicates some remaining air at or below the residual gas saturation of 1% that was assumed for the EBS materials. In general, the model reproduced reasonably well the observed pressure and saturation response in the different sand/bentonite layers. The results indicate significantly higher permeabilities for the sand/bentonite Layers 8 – 10 compared to the other layers. This is probably due to the addition of the lead-nitrate in the sand/bentonite mixture, which limits swelling of the bentonite between the sand grains (Romero et al., 2002). However, significant uncertainty remained with regard to the variability of the saturation response within individual layers and limited constraint on the permeability of the high-K layers and associated conceptual model for the sand/bentonite.

Prior to the gas injection stage of the in-situ experiment, a series of water tests was designed, which were conducted between October and December 2002. The observed pressure response of the water test (WT1) was then analyzed with iTOUGH2 to calibrate the hydraulic properties and assess the degree of saturation of the sand/bentonite.

WATER TEST (WT1)

WT1 consisted of a series of test sequences, shown in Figure 7. The measured pressures during WT1 indicate distinct hydraulic pressure responses between the silo and the high-K sand/bentonite layers, both for the constant rate injection (RI) and withdrawal (RW) tests, as well as for the sinusoidal extraction from the silo (RWSin1) and for the sinusoidal injection into the upper cavern (CVRISin1). Following the CVRISin1 sequence and a subsequent recovery period (Fig. 6), short gas injection tests (GT1) were performed to test the equipment for the gas injection phase and to provide a preliminary assessment with the TOUGH2 design model for simulating different gas injection rates and injection strategies.

During WT1 water injection into the upper cavern continued, which is monitored by the pressure at the base of the upper cavern. The pressure response shows some variability caused by fluctuations in the water injection rates. These pressure changes in the upper cavern also induced distinct responses in the sand/bentonite in Layers 8 – 10 as well as in the silo, indicating a well-connected hydraulic system. The pressures in Layer 8 also show a distinct response to the induced pressure changes in the silo, particularly during RW1.
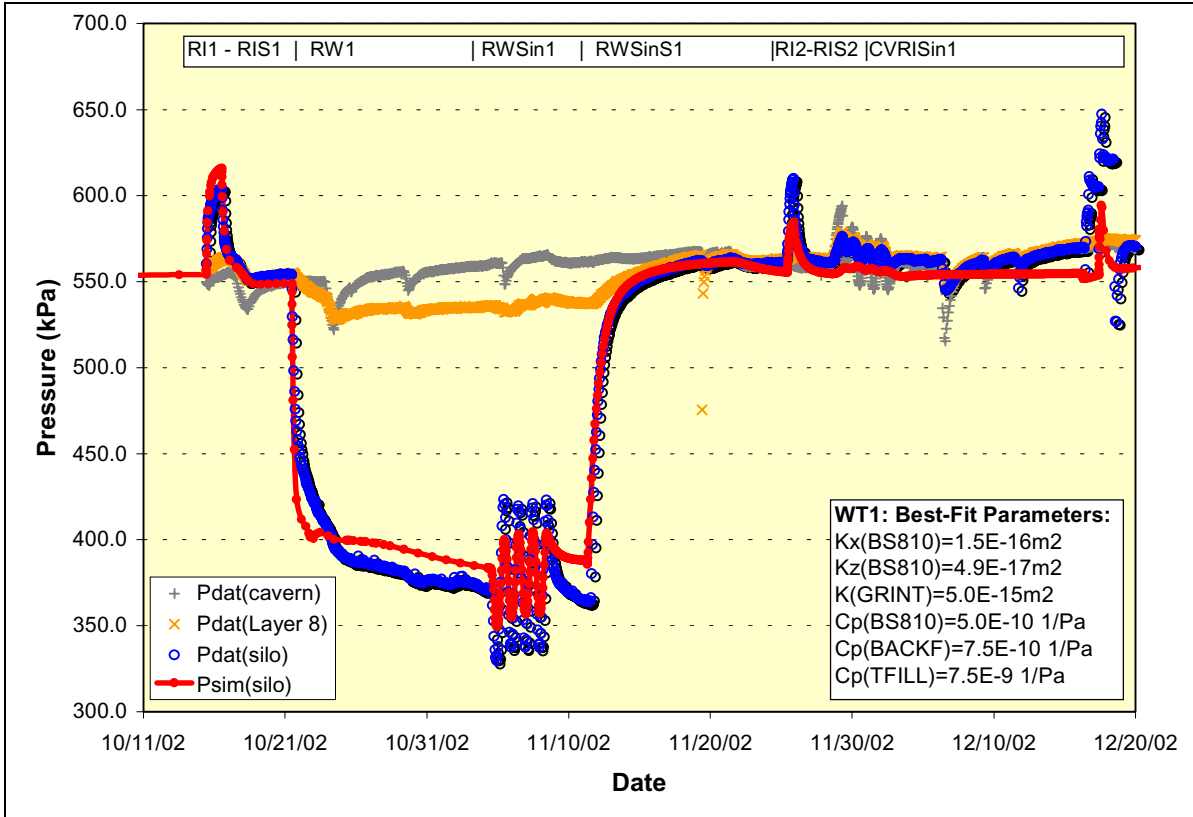
Figure 6. Measured pressure response in the silo, in Layer 8 (high-K) and in the cavern upper. Simulated silo pressure is based on the best-fit parameters for the entire WT1 sequence.
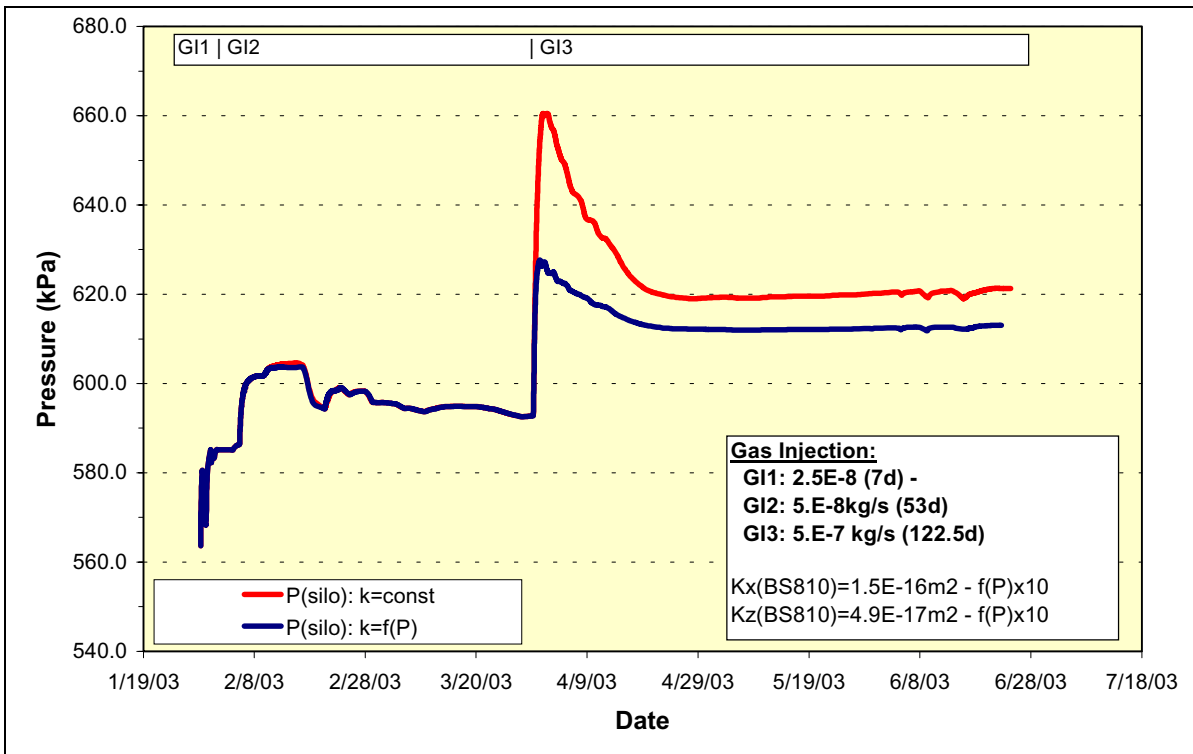

Figure 7. Simulated injection pressure for the gas injection phase for two cases assuming (a) constant permeability, and (b) pressure-dependent permeability of the sand/bentonite in Layers 8 – 10.

The analysis of the individual WT1 sequences was complemented by analytical and numerical well test analyses. The well-test analysis results indicated noticeably higher permeabilities (based on 1-m radial layer thickness) for the RI1-RIS1 sequence ($k=1.6E-16$ m^2) compared to the RW1 and the RI2 sequences ($k=5.0E-17$ m^2).

Initial conditions for the simulation of the WT1 sequence were based on the saturation simulations described above, representing pressure and saturation conditions at the end of September 2002. The WT1 simulations included a 15 day equilibration period prior to the start of the RI1 sequence (Oct. 15) to allow for adjustment to the updated hydraulic properties.

Compared to the saturation simulations described above, the pressure in the upper cavern was controlled by the water injection rate, incorporating the sudden declines during RI1-RW1 (Fig. 6). These represent distinct pressure signals which could be detected in the sand/bentonite and in the silo. In addition to the injection rate the pressure in the upper cavern is controlled by leakage into the rock laboratory tunnel, which indicated a decreasing outflow during the saturation phase and, to a certain extent, during WT1. This decline resulted in a gradual pressure increase in the upper cavern, and the water injection was periodically adjusted to lower rates. The decline in leakage was accounted for in the modeling by step-wise reduction in the permeability assigned to the tunnel seal.

The TOUGH2 modeling of the WT1 sequence was performed in several steps using inverse simulations of specific tests for parameter estimation and forward simulations for the entire WT1 sequence that is shown in Figure 6. Similar to the saturation stage analysis, the two conceptual models for the sand/bentonite for Layers 8 – 10 were considered in different simulations. The silo pressure response with the "base-case" parameter set (Fig. 6) was based on the uniform-K model, although either conceptual model had advantages and disadvantages in reproducing the different WT1 test sequences.

As mentioned above, the well-test analysis indicated lower permeability for the RW1 event compared to the RI1 event. iTOUGH2 runs corroborated that the calibrated permeabilities from the RW1 sequence resulted in a larger pressure buildup for RI1 (Fig. 6), indicating a higher permeability for RI1. On the other hand, the same permeability estimates produced a much lower pressure buildup during RI2, suggesting a decrease in permeability.

Another important parameter controlling the potential dissipation of the pressure signals between the upper cavern and the silo is the compressibility of the system represented by the pore compressibility and saturation. The iTOUGH2 simulations of the RW1 sequence for the uniform-K model yielded unrealistically low pore compressibility for the sand/bentonite Layers 8 – 10 when calibrating to pressure data from both the silo and Layer 8. Despite these low values the distinct pressure fluctuations in the upper cavern during RI1-RW1 are only vaguely reproduced in the simulated silo pressures. This suggests that the gas saturation in the sand/bentonite Layers 8 – 10 at the start of WT1 or during the RW1, due to degassing of dissolved gas associated with the pressure decline, is too high resulting in high bulk compressibilities, which are offset in the iTOUGH2 calibration by extremely low pore compressibilities.

Alternatively, instead of the radial flow geometry for the upper sand/bentonite layers, more localized pathways for hydraulic communication between the silo and the upper cavern would be required to reproduce the rapid pressure response in the silo due to sudden changes in the upper cavern pressure. The corresponding iTOUGH2 simulations using the high-K tops model did not require such extremely low compressibility, but the overall fit for the RI1-RW1 sequence was relatively poor due to a distinct offset in the silo pressure that occurred during the equilibration period prior to the start of WT1.

The base-case parameter set reproduced reasonably well the entire WT1 sequence, but indicated several limitations. The RW1 sequence is apparently affected by two-phase flow conditions, which suggests possibly too high a remaining gas saturation at the start of WT1, or that the implementation of two-phase flow processes and associated assumptions within the numerical model are too simplified to describe the detailed processes occurring within the silo and in the nearby sand/bentonite during the test. Also, the simulated injection pressure buildup for RI2 is lower, suggesting possible changes in permeability between RI1 and RI2 and that the permeability may be on the low side for the subsequent gas injection phase.

The WT1 analysis is considered preliminary and will be further examined to take into account possible changes in the pressure offsets based on recalibration of the pressure transducers. Overall the model reproduced reasonably well the WT1 sequence and was used for the design of the gas injection phase described below.

GAS INJECTION DESIGN

For the main gas injection test, a series of simulations were performed with the design model, evaluating different injection strategies. A major concern is the relatively low confining stress (possibly ca. 40 kPa), which could cause pathway dilation in the sand/bentonite or opening of interfaces at the concrete – sand/bentonite contact when the gas pressure approaches or exceeds the confining stress. The gas injection design simulations used the base-case parameter set derived from the preliminary WT1 analysis, described above. The gas injection rates, which were ultimately used in the in-situ test, used a step-wise increase starting at a relatively low rate of 2.5E-8 kg/s for 7 days, which is increased to 5.E-8 kg/s for 53 days, and will be ultimately increased to 5.E-7 kg/s. The injection pressure response is shown in Figure 7 for two cases, (1) assuming constant permeability of the sand/bentonite Layers 8 – 10, and (2) assuming a pressure-dependent permeability when the injection pressure exceeds the confining stress (i.e. injection pressure of 600 kPa).

The simulations indicate that for both cases gas does not start to migrate into the sand/bentonite at the lowest gas injection rate (GI1). During GI2, gas starts to migrate into the sand/bentonite after Feb. 17th, indicated by a sudden pressure drop followed by a smaller pressure increase (Fig. 7). Overall, however, the injection pressure declines during GI2. The increase in gas injection during GI3 shows a steep pressure rise, followed by a decline which levels off to approximately constant pressures. The two cases differ mainly during GI3, indicating lower peak pressure for the case assuming pressure-dependent permeability, as the permeability of the sand/ bentonite above the silo increased.

SUMMARY

A numerical model was implemented with TOUGH2 to design the different stages of the GMT experiment and to analyze the resulting data from the saturation and WT1 stages. iTOUGH2 modeling was used for parameter calibration and to assist in the understanding of the overall system behavior. The analysis results were ultimately used for developing an optimized gas injection strategy which is currently being implemented in the in-situ experiment.

REFERENCES

Finsterle, S., iTOUGH2 User's Guide, Version 2.2, Lawrence Berkeley National Laboratory Report, LBL-34581, Berkeley, CA, 1993.

Lanyon, G.W., GMT/IR 00-01 Laboratory data compilation report. Nagra NPB 00-20, 2000.

Pruess, K., C. Oldenburg, and G. Moridis, *TOUGH2 User's Guide, Version 2.0*, Report LBNL-43134, Lawrence Berkeley National Laboratory, Berkeley, Calif., 1999.

Romero, E., Alonso, E.E., Knobelsdorf, J., GMT/IR 02-02: Laboratory tests on compacted sand/bentonite buffer material for the GMT in-situ emplacement. Nagra NPB 02-05, 2002

Romero, E., Castellanos, E., Alonso, E.E., GMT/IR 02-01: Laboratory tests on compacted sand/ bentonite/ lead nitrate buffer material for the GMT emplacement project. Nagra NPB 02-24, 2003.